 doi:10.20944/preprints202101.0439.v1

Article

The change P82L in the Rift Valley fever virus NSs protein confers attenuation in mice not related with a type-I IFN antagonistic phenotype

Belén Borrego [1]; Sandra Moreno [1]; Nuria de la Losa [1]; Friedemann Weber [2]; Alejandro Brun [1,*]

[1] Centro de Investigación en Sanidad Animal, INIA-CISA, Valdeolmos, Spain
[2] Institut für Virologie, Justus-Liebig-Universität Giessen, Germany
* Correspondence: brun@inia.es

Abstract: Rift valley fever virus (RVFV) is a mosquito-borne bunyavirus that causes an important disease in ruminants, with great economic losses. The infection can be also transmitted to humans; therefore it is considered a major threat to both human and animal health. In a previous work, we described a novel RVFV variant selected in cell culture in the presence of the antiviral agent favipiravir that was highly attenuated in vivo. This variant displayed 24 amino acid substitutions in different viral proteins when compared to its parental viral strain, two of them located in the NSs protein that is known to be the major virulence factor of RVFV. By means of a reverse genetics system, in this work we have analyzed the effect that one of these substitutions, P82L, has in viral attenuation in vivo. Rescued viruses carrying this single amino acid change were clearly attenuated in BALB/c mice while their growth in an IFN-competent cell line as well as the production of IFN-β did not seem to be affected. However, the pattern of nuclear NSs accumulation was modified in cells infected with the mutant viruses. These results unveil a new RVFV virulence marker highlighting the multiple ways of NSs protein to modulate viral infectivity.

Keywords: Rift Valley fever virus; non-structural NSs protein; interferon antagonist; nuclear filaments; PXXP motifs.

1. Introduction

Rift valley fever virus (RVFV) is a mosquito-borne phlebovirus of the *Phenuiviridae* family (O. *Bunyavirales*) that causes an important disease in ruminants, mostly characterized by a high-rate of abortions, fetal malformation and death of newborn lambs, with great economic losses. The infection can be transmitted to humans through mosquito bites or when exposed to infected material, producing a usually self-limiting disease with more severe development in a low percentage of cases (reviewed in [1]). Rift Valley fever is confined to the African continent and Southern parts of the Arabian Peninsula and Indian Ocean islands, but its potential for spreading to other geographical areas linked to climatic change and globalization has been widely remarked [2]. Veterinary vaccines are available in Africa, but currently there are no licensed vaccines for human use, while in Europe there is no available treatment or licensed RVF vaccine. Therefore, developing of safer and effective control strategies intended also for human use is an active field of research [3-5].

The RVFV genome consists of three ssRNA(-) segments of different size (Large, Medium, Small). The L-segment codes for an RNA dependent RNA polymerase (RdRp). The M segment contains five in-frame start codons alternatively used by virtue of a ribosomal "leaky scanning" mechanism for the synthesis of the envelope glycoproteins (Gn and Gc), a cytosolic accessory protein (NSm) that can be found in two isoforms of 13-14-kDa protein [6], and a 78-kDa glycoprotein (NSm-Gn) that incorporates in virus particles when produced in insect cells [7] but with unknown function in mammal hosts. The S segment

encodes in an ambisense strategy the viral 27kDa nucleoprotein (N), and a 30kDa protein (NSs), considered the main virulence factor of the virus.

The NSs protein inhibits the host antiviral responses by multiple pathways that, either alone or combined, allow the virus to replicate efficiently. NSs interaction with several binding partners promotes the sequestration or degradation of a number of cellular proteins thus avoiding their functions: NSs prevents activation of the IFN-ß promoter, promotes degradation of double-stranded RNA-dependent protein kinase R (PKR) and blocks the assembly of transcription factor II H (TFIIH) inducing a general transcription shut off in infected cells (reviewed in [8] and [9]). These biological functions seem to be dependent on the nuclear localization of NSs in the infected cells, where it assembles displaying a typical filamentous pattern unique in phleboviruses. Another role related with the accumulation of superoxide in infected cells has been suggested for NSs, in association with non-nuclear compartments, such as mitochondria [10]. Several works identified different amino acid positions or regions of the protein involved in different functions. An essential core domain spanning residues 83–248 was shown to be sufficient for filament formation [11]; other results suggest that the NSs functionality is more likely dependent on conformational integrity than on the presence of particular domains [12]. However, the understanding of the whole picture is still unclear, especially regarding the relationships between some of these functions and their combined contribution to virulence in vivo. Characterization of the biological features of NSs is a big step towards the development of effective control measures for RVF. Due to its role providing an efficient viral replication, NSs appears to be a good target for antivirals and, in addition, some attenuated live vaccines are based on viruses lacking or carrying a non-functional NSs protein. Besides these biological functions, recent data showed that the reported nuclear NSs filamentous pattern corresponds to amyloid-like structures that could play an important role in mouse neuropathology or neurotoxicity [13].

In a previous work aimed to characterize a novel RVFV variant that was selected in cell culture in the presence of the antiviral compound favipiravir, we found that this virus, named as 40F-p8, was highly attenuated in vivo [14]. Out of the 24 amino acid substitutions found in other viral proteins when compared to the parental virulent strain, only two changes were located on the NSs protein: V52I and P82L. Since V52I is a conservative substitution and variants at this position have been reported in other RVFV strains (V52A in Madagascar strains 0212-08 and 200803162) we focused in the P82L mutation. P82 is placed within the PXXP motif 2 (positions 82 to 85), a motif reported to be involved in both NSs nuclear localization and IFN-β activation/expression, with proline residues playing a critical role [15]. In this work, using a reverse genetics system, we investigated the role of NSs P82L mutants on the viral infectivity in vivo in a mouse model of infection.

2. Materials and Methods

Cells

The cell lines used for this study were HEK293T (human embryonic kidney 293 cells, ATCC CRL-3216), Vero (African green monkey kidney cells, ATCC CCL-81) and BHK-21 (baby hamster kidney fibroblasts, ATCC CCL-10). All cell lines were grown as described [16]. rRVFV previously generated (rZH548 (wild-type) and a NSs-deleted virus expressing green fluorescent protein, named as rZH548ΔNSs::GFP, [16]) were included as controls in the different assays. Infections and titrations were performed as described [14].

The levels of human IFN-beta in infected HEK293 cell supernatants were tested by ELISA using a commercial PBL Assay Science kit, following manufacturer's instructions.

Rescue of recombinant viruses

Recombinant RVF viruses were rescued by means of a reverse genetic system [16, 17]. Briefly, this system is based on transfection of HEK293 and BHK-21 cell co-cultures of

 doi:10.20944/preprints202101.0439.v1

a set of 5 plasmids comprising 3 plasmids providing viral genomic segments L, M and S (pHH21_RVFV_vL, pHH21_RVFV_vM and pHH21_RVFV_vS respectively) and 2 plasmids providing the viral polymerase L and the nucleoprotein N (pI.18_RVFV_L and pI.18_RVFV_N).

To generate the plasmid carrying a mutant S segment, the desired nucleotide change C279T (numbering according to NC_014395 RVFV segment S, strain "ZH-548") was introduced in plasmid pHH21-RVFV-vS by PCR using the Q5® Site-Directed Mutagenesis Kit (NewEngland Biolabs) following manufacturer´s protocols. The primers used, designed using the NEB online design software NEBaseChanger™, were S279Fwd (5'-GCACCTCCACTAGCGAAGCCT-3'; underlined letter corresponds to the nucleotide changed) and S279Rev (5'-AACGTTTGATGCAAAGTCTCCAAGTC-3'). On days 3, 5 and 7, transfected cell supernatants were harvested and inoculated onto BHK-21 cells in order to screen for the presence of mutant virus by cytopathic effect (CPE). For those rendering positive CPE, further two passages were performed to generate a virus stock for use in the present experiments.

Sequencing

RNA was extracted from the supernatants of infected cells or blood samples as described [16]. Amplicons corresponding to the NSs ORF were obtained by RT-PCR and sequenced as described [14].

Animal inoculation and sampling

BALB/c mice (9-18 week-old male) were used for the in vivo studies. They were equally distributed into groups of 5-7 animals and inoculated intraperitoneally with 500 plaque-forming units (pfu) of the corresponding viruses. Development of disease was evaluated daily over 3 weeks (18 days) in terms of morbidity and mortality as described elsewhere [18]. Blood samples were taken by submandibular puncture at 72 h after infection and tested for viral RNA by RT-qPCR [16,19] to monitor viremia, while serum samples collected from survivor mice at the end of the experiment (day 18 pi) were used in antibody assays. Mice were housed in biosafety level 3 (BSL-3) animal facilities at INIA-CISA before use. All experimental procedures involving animals were performed in accordance with EU guidelines (directive 2010/63/EU), and protocols approved by the Animal Care and Biosafety Ethics' Committees of INIA and Comunidad de Madrid (permit codes CEEA 2014/26, CBS 2017/15, PROEX 108/15 and PROEX192/17).

Antibody assays

Antibodies against NP were detected by an in-house ELISA and RVFV neutralizing antibodies in a microneutralization assay [14]. Anti-NP titers are expressed as last dilution of serum (log10) giving an OD reading at 450 nm over 1.0 in ELISA; neutralization titers are expressed as the dilution of serum (log10) rendering a reduction of infectivity of 50%.

Immunofluorescence

Vero cells were infected at a MOI of 1 and, at the time post-infection (pi) indicated, cells were fixed with 4% paraformaldehyde and subjected to indirect immunofluorescence with the anti-NSs monoclonal antibody 5C3A1B12 [20] kindly provided by Dr. Martin Eiden (Friedrich-Loeffler Institute. Riems, Germany) following procedures as described [16]. All the buffers included 0.1% saponin for permeabilization. Secondary antibody was a goat anti-mouse Alexa Fluor 488. Cell nuclei were stained with DAPI. Microscopy was performed with a Zeiss LSM880 confocal laser microscope. The size of the NSs aggregates visualized was analyzed with ImageJ/Fiji software. Briefly, after subtracting background, particles of higher size were selected by applying a threshold inside the cell nucleus trying to discriminate for filamentous structures. Then an "Analyze Particles" was performed (in at least two images per sample), and the average size of the particles determined.

 doi:10.20944/preprints202101.0439.v1

Western blot

HEK293 cells were infected at a MOI of 1.0 and whole cell extracts harvested at 20 hpi were analyzed by western blot using anti-PKR (B-10) and anti-p62 (H10) mouse monoclonal antibodies (SantaCruz Biotechnology), anti RVFV-N mAb 2B1 [16] and mouse anti-actin antibody (Sigma) as primary antibodies. Loaded samples correspond to 10^6 cells per well.

Statistical analysis

Data analysis was performed using GraphPad Prism software (version 6.0). Differences in survival times were tested by the Log-Rank (Mantel-Cox) test. Variations in mean viral titers were analyzed using non-parametric one-way ANOVA test (Kruskall-Wallis test) with Dunn's multiple comparison post-hoc tests. Differences were considered statistically significant when $p < 0.05$.

3. Results

3.1. Rescue of recombinant Rift Valley fever viruses carrying the S279 substitution

We planned to rescue recombinant ZH548 (rZH548) viruses carrying the amino acid substitution P82L in the NSs protein by means of our reverse genetic system [17]. This amino acid change was deduced from the nucleotide sequence of the virus 40F-p8 that displayed the change C279T in the corresponding codon (CCA in the parental virus RVFV 56/74, CTA in the selected variant; [14]). Thus, we first introduced the desired nucleotide change C279T in the plasmid corresponding to genomic S-segment, pHH21-RVFV-vS. After checking the correct sequence of the resulting plasmid, co-cultures of HEK293 and BHK-21 cells were transfected in triplicates. At days 3, 5 and 7 post-transfection supernatants were harvested and inoculated onto BHK-21 cells in order to screen for the presence of mutant virus by the appearance of cytopathic effect (CPE). In samples collected at days 5 and 7 post-transfection from 2 separate replica wells total CPE was observed at day 4 pi. Viruses were grown on BHK-21 cells for 3 passages, with CPE registered at 48 hpi and yields of 8.4- and 3.2x 10^7 pfu/ml, comparable to the wt rZH548 (2.7x 10^7 pfu/ml). Plaque formation on Vero cells was indistinguishable of rZH548 (not shown). The presence of the mutation was confirmed by RT-PCR amplification of genomic S-segment and further sequence analysis and no other changes were detected in the NSs gene. Viruses were generically named after the nucleotide position changed (rZH548-mut S279 viruses). In particular, the two viruses obtained after 3 passages were termed 2B7 and 3VB5 and are the viral clones used for this study.

3.2. Analysis of infectivity and immunogenicity of recombinant rZH548-mut S279 viruses in mice

The virulence of the recombinant rZH548-mut S279 viruses was tested in BALB/c mice by IP inoculation of 500 plaque-forming units (pfu) of the two rescued viruses, 2B7 and 3VB5. Rescued rZH548 (wild-type) and a NSs-deleted virus expressing green fluorescent protein, named as rZH548ΔNSs::GFP, were included as controls for virulence and attenuation, respectively (figure 1).

Preprints (www.preprints.org) | NOT PEER-REVIEWED | Posted: 22 January 2021 doi:10.20944/preprints202101.0439.v1

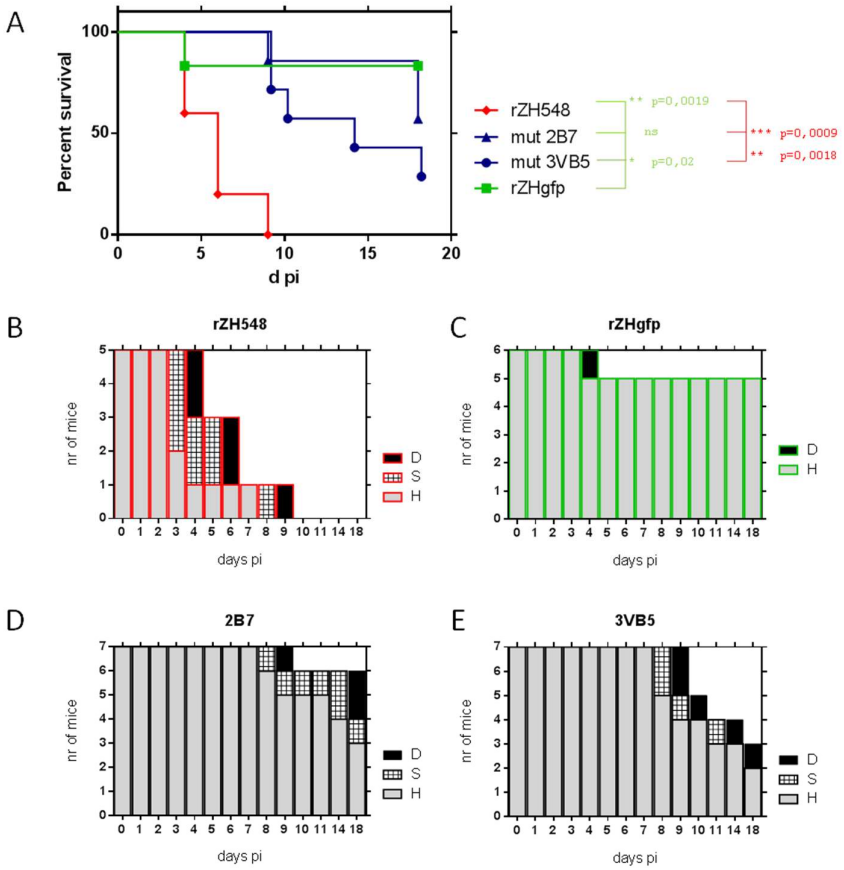

Figure 1. Analysis of the in vivo infectivity of the rZH548-S279 mutant viruses in BALB/c mice. 9-16 week-old male mice (n=5 -7, equally distributed) were inoculated IP with 500 pfu of the indicated viruses: the two rZH548-mut S279 viruses 2B7 and 3VB5. Wild-type rZH548 (red) and rZH548ΔNSs::GFP (labeled as rZHgfp, green) viruses were included as controls for virulence and attenuation, respectively. Animals were monitored daily during 18 days. (A) Survival rates and (B-E) Morbidity upon challenge with the indicated viruses. The graph represents the clinical status of each mouse: D (dead/euthanized): black bars; S (signs-sick), hatched bars; H (healthy), grey bars. The animal within the group rZH548ΔNSs:GFP euthanized at day 4 pi was excluded from the survival analysis.

In the control group inoculated with the attenuated, NSs-deleted, rZH548 virus one mouse showed, unexpectedly, tremors and a severe weight loss (20%) one day after bleeding and was euthanized (day 4). We considered that this mouse did not recover well from the stress caused by the bleeding procedure and was excluded from the statistical analysis, thus a 100% survival was considered for this group. No signs of disease were observed in any animal within this group.

In mice inoculated with wt rZH548, first signs of disease (watery eye, reduced mobility, ruffled fur) appeared at day 3 with first deaths occurring at day 4; disease evolved rapidly (hunched back, lethargy, paralysis) and at day 9 all the animals had deceased. Median survival time of this group was 6 days. In contrast, animals inoculated with the rZH548-mut S279 viruses remained without signs of disease the first week after inoculation, when disease signs were first observed. At the end of the experiment (day 18 pi) these groups recorded significantly higher survival rates: 2 out of 7mice inoculated with 3VB5 survived, with a median survival time of 14 days. In the group inoculated with

Preprints (www.preprints.org) | NOT PEER-REVIEWED | Posted: 22 January 2021 doi:10.20944/preprints202101.0439.v1

2B7 the survival percentage was slightly increased (4 out of 7) but this apparent difference did not reach statistical significance (p=0.1991), as judged by the LogRank (Mantel-Cox) test.

Viral loads at day 3 were analyzed by RT-qPCR (figure 2A). As expected, all samples recovered from mice inoculated with rZH548 revealed high viral loads, while viral RNA in samples from rZH548ΔNSs::GFP-immunized mice was below the detection level. In mice immunized with rZH548-mut S279 viruses viral loads at day 3 pi were strongly reduced, with one animal rendering also undetectable RNA levels (2B7 group). Viral RNA recovered from some randomly selected samples was also used for RT-PCR amplification and sequencing of the NSs ORF, confirming the presence of the mutation and no other changes.

These results of viremia correlated with the levels of seroconversion to viral proteins detected in survivor mice (figure 2B). Anti-NP antibodies, indicative of viral replication, were detected in all mice, including also those inoculated with rZH548ΔNSs::GFP virus where no viral RNA was detected. Likewise, antibodies able to neutralize RVFV infectivity in vitro were detected in all animals. Compared to those reached in the rZH548ΔNSs::GFP group, titers in both assays were slightly higher in groups inoculated with the rZH548-mut S279 viruses, although these differences were not statistically significant (one-way ANOVA test).

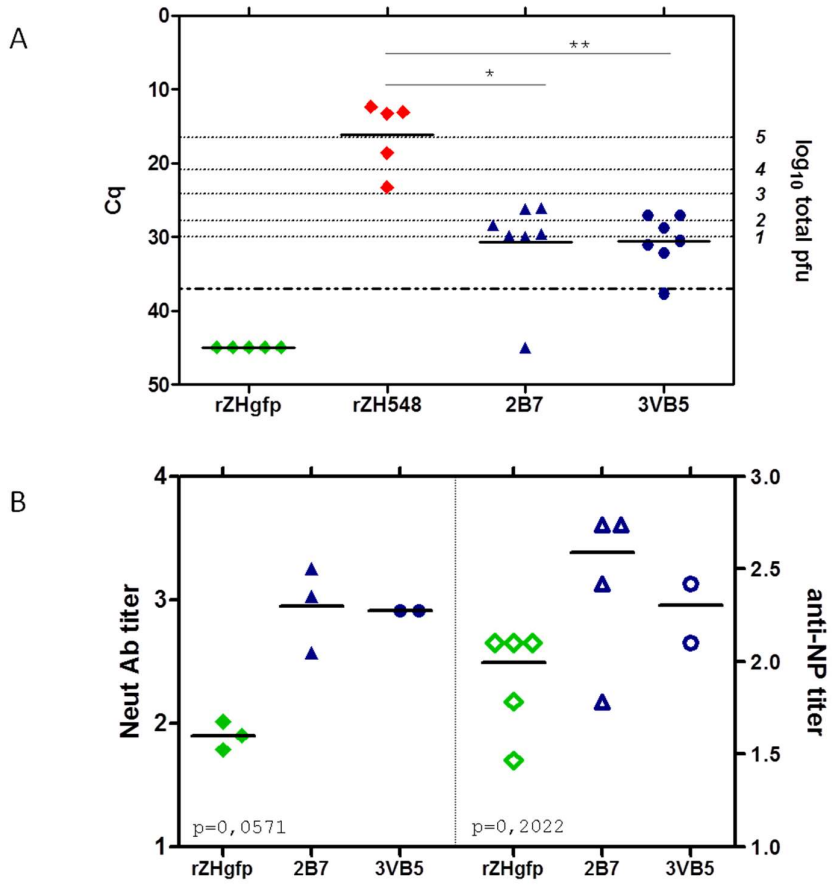

Figure 2. Viremia and seroconversion after inoculation with the rZH548-S279 mutant viruses. (A) Viremia. RT-qPCR on EDTA blood samples collected at day 3 pi. Samples giving a Cq value under the detection level of the assay, 37, are arbitrarily represented as 45 and were excluded from

 doi:10.20944/preprints202101.0439.v1

the statistical analysis. (B) Antibody responses in survivor mice at day 18 pi. Titers are expressed as dilution of serum (log10) rendering a reduction of infectivity of 50% in a microneutralization assay (left Y-axis; closed symbols), and last dilution of serum (log10) giving an OD reading at 450 nm over 1.0 in anti-NP ELISA (right Y-axis; open symbols). Each symbol corresponds to an individual mouse. For neutralization, only n=3 samples were available for rZH548ΔNSs::GFP and 2B7. *p ≤ 0.05, **p ≤ 0.001.

3.3. Cellular localization and pattern of NSs in cells infected with rZH548-S279-mutants

Once proved that the change P82L introduced in the NSs led to attenuation of RVFV in mice, we performed some *in vitro* assays to further characterize the phenotype of the S279-mutant viruses. First, we tested the pattern of cellular distribution of the mutated NSs in Vero-infected cells. P82 is placed within PXXP motif 2 (positions 82 to 85), and changes in two of the four PXXP motifs present in the NSs (motif 1 at positions 29 to 32, and motif 2 at positions 82 to 85) are known to affect the nuclear filamentous arrangement of NSs, with NSs mutants remaining in the cytoplasm [15]. In order to test whether the change P82L carried by our S279-mutants affected this pattern, infected Vero cells were subjected to indirect immunofluorescence with the anti-NSs monoclonal antibody 5C3AB12 [20]. At 6 h pi, NSs could be detected in the cytoplasm of all infected cells in all cases, but in the nucleus the prototypical fibrillar NSs structures could only be detected after infection with wt rZH548 virus (figure 3A, left panels). In contrast, in cells infected with the NSs-mutant viruses, this typical nuclear staining was harder to find at this early point and, when present, filaments seemed less defined. Rather, the fluorescence had a punctate pattern distributed along the cytoplasm and the cell nucleus. At 24 h pi filamentous structures could be detected in the nucleus in all cases, although some subtle morphologic differences were found again between filaments formed in cells infected with the wt and the NSs-mutant viruses (figure 3A, right panels). While in rZH548-infected cells nuclear filaments appeared thicker and sharply defined, those in cells infected with both rZH548-mut S279 viruses looked more disordered and loosely aggregated and with more cytoplasmic staining.

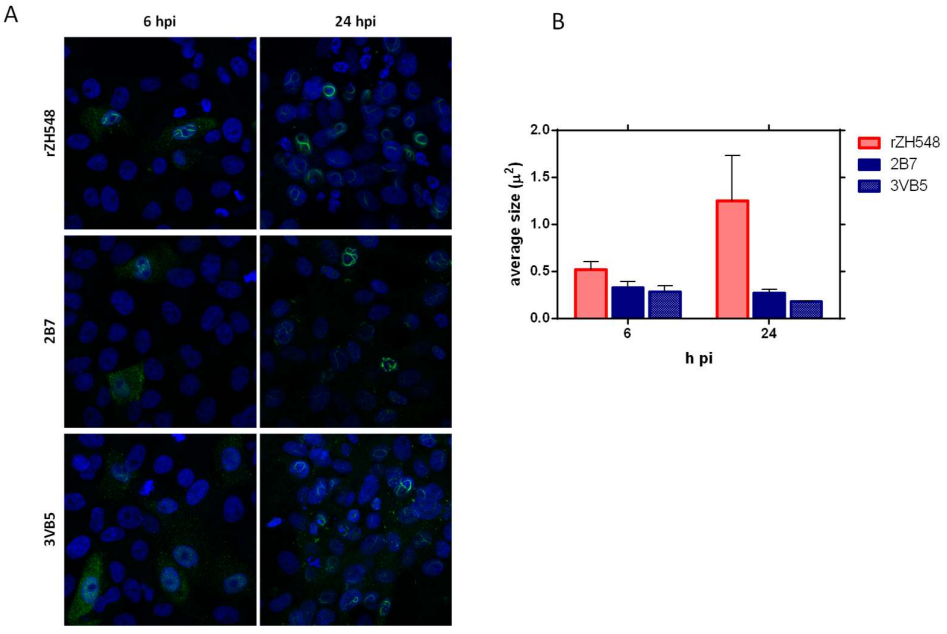

Figure 3. Localization and filament formation of wt and mutant NSs proteins. (A) Vero cells were infected with rZH548 and the two rZH548-S279 mutants at a MOI of 1. At 6 (left panels) and 24 (right panels) hours pi cells were fixed and subjected to indirect immunofluorescence with the

 doi:10.20944/preprints202101.0439.v1

anti-NSs monoclonal antibody 5C3A1B2. Nuclei were stained with DAPI. Upper panels: infection with rZH548 virus; central panels: infection with mutant virus 2B7; lower panels: infection with mutant virus 3VB5. (B) Size estimation of the nuclear NSs aggregates in infected cells. The average size of intranuclear NSs aggregates was determined using ImageJ software. At least two images were analyzed per sample.

In an attempt to quantify this observation, we analyzed the size of the observed NSs aggregates and determined the average size of the particles (figure 3B). In rZH548-infected cells, average size of the NSs particles was higher and increased with time, while in cells infected with both rZH548-mut S279 viruses the average size was lower and remained so at 24 h pi, probably reflecting the higher number of particulate structures that do not aggregate in cells infected with mutant viruses.

3.4. Growth and IFN-β induction of rZH548-S279 mutants on HEK293 cells

NSs is an antagonist of the antiviral type I interferon (IFN) system. RVFVs lacking NSs or a functional NSs are unable to counteract the IFN response, thus showing an impaired growth in interferon-competent cells [21] [15,22]. As for the nuclear pattern of NSs, changes in the PXXP motifs have also been reported to affect the ability to suppress the activation of IFN-β promoter, in particular when prolines were substituted [15]. Thus, we decided to check whether the change P82L had some effect on the growth of rZH548-mut S279 viruses on interferon-competent HEK-293 cells. Both the rZH548ΔNSs::GFP and the wt rZH548 virus were again included for a comparison as examples of IFN-sensitive or non-sensitive viruses, respectively (figure 4). As expected, titers of the rZH548ΔNSs::GFP did not increase over time. In contrast, the growth curves of the two S279-mutant viruses were similar to the one displayed by the wt rZH548 virus, showing increasing titers along the time analyzed. In addition, these supernatants were analyzed for the presence of human IFN-β by ELISA. IFN-β was only detected in samples recovered 48 hpi from cells infected with rZH548ΔNSs::GFP. All the other samples rendered OD values corresponding to IFN levels below or close to the sensitivity threshold of the assay (50 pg/ml). Altogether, these results suggested that the single P82L change introduced in rZH548-mut S279 viruses did not affect the ability of NSs to block the cellular production of IFN and thus their growth in these IFN-competent cells.

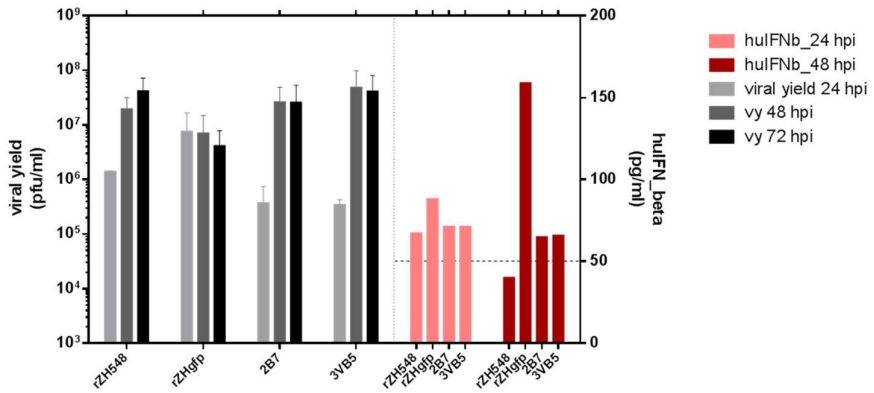

Figure 4. Growth of rZH548-S279 mutants on HEK293 cells and IFN-β production. HEK293 cells were infected at a MOI of 0.05 with the indicated viruses. At 24, 48 and 72 hpi, supernatants were collected and titrated on Vero cells (grey-black bars); samples collected at 24 and 48 hpi were also analyzed for IFN-β production by ELISA (red bars).

 doi:10.20944/preprints202101.0439.v1

3.5. Degradation of PKR and p62 in rZH548-S279- infected cells

Another pathway by which NSs blocks the host antiviral responses of infected cells is the degradation of cellular proteins such as PKR and p62, a component of transcription factor II H (TFIIH) [23-25]. In order to determine whether the change P82L affected this ability and could therefore modulate viral attenuation, HEK293 cells were infected and whole cell extracts analyzed by western blot (figure 5). In samples from cells infected with the two rZH548-S279-viruses, the expression of PKR was clearly diminished while p62 was undetectable, suggesting that the change P82L did not impair the ability of the mutant protein to degrade the cellular proteins under study.

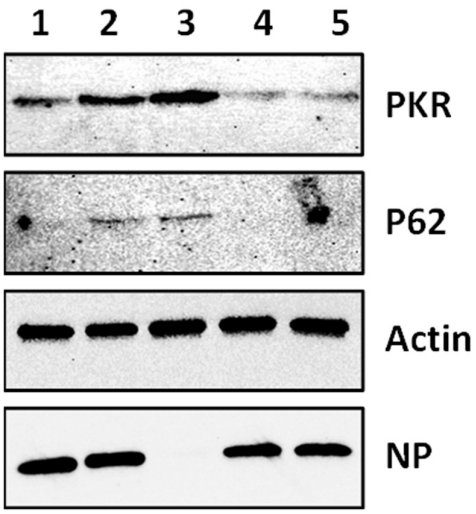

Figure 5. Degradation of PKR and p62 in rZH548-S279 infected cells. HEK293 cells were infected at a MOI of 1 with rZH548 (lane 1), rZH548ΔNSs::GFP (lane 2) and the two rZH548-S279 viral clones generated in this work (3VB5 and 2B7, lanes 4 and 5 respectively). Lane 3 corresponds to mock-infected cells. Cells were harvested at 20 hpi and analyzed by Western blot using anti-PKR (B-10), anti-p62 (H10) mouse monoclonal antibodies, anti RVFV-NP mAb 2B1 and anti-actin antibody as primary antibodies. Samples loaded correspond to 10^6 cells.

4. Discussion

In this work we describe the rescue of recombinant ZH548 (rZH548) RVF viruses carrying a P82L mutated NSs protein and analyze the effect of this change in RVFV infectivity. This mutation was originally identified in a virus isolated under the selective pressure of a mutagenic agent and found later to be hyper-attenuated in mice [14,26]. Apart from other amino acid substitutions identified in this RVFV variant, it was especially interesting to study those found in the NSs protein, known to be the main virulence factor for RVFV. The substitution of proline 82 was particularly interesting since it lies within a PXXP motif involved in the correct nuclear localization of the protein and in the ability to suppress IFN-β promoter activation [15].

When viruses carrying P82L NSs were tested in vivo, viral loads were reduced, disease appeared later than in controls and survival rates were higher, confirming that this substitution led to virus attenuation in mice. Surprisingly, none of the in vitro assays performed revealed a clear difference between rZH548wt and rZH548-mut S279 viruses: they all were able to grow in IFN-competent HEK293 cells and block the cellular production of IFN-β retaining the ability to degrade both PKR and p62 proteins.

The only feature where we identified a slight difference between the wt and the S279-mutant viruses was the pattern of nuclear distribution of NSs in infected cells. Even though filamentous structures were observed in the nucleus in all cases, the assembly of

these typical structures was somehow impaired for the mutant NSs, appearing with some delay and with a more loose consistency at later times pi, suggesting some deficiency in the aggregation capability or kinetics. It is difficult to determine whether this is an actual trait with any effect on the NSs activities, not only in vitro, but especially in vivo. Correlation between this typical pattern of RVFV NSs and in vivo virulence is controversial since it was described that nuclear filament formation is important but not sufficient for in vivo virulence [27, 28]. Interestingly, recent data reported that the nuclear NSs filamentous pattern indeed corresponds to amyloid-like structures, therefore stressing the potential role of NSs in mouse neuropathology or neurotoxicity [13]. Further work is needed to assess the role of the P82L change in amyloid formation.

Our results provide some noteworthy findings for the development of live attenuated vaccines. In terms of attenuation, the substitution of residue P82L has a remarkable effect in mice, with higher survival than the wt virus. Most animals infected with S279-mutant viruses developed detectable viremia and strong seroconversion to RVFV, both at higher levels than mice inoculated with attenuated ΔNSs virus expressing green fluorescent protein (rZH548ΔNSs::GFP). When developing safer and more stable live-attenuated vaccines, a whole deletion provides a better approach than single amino acid substitutions, with lower chances of changes and reversion. Nonetheless, a total lack of NSs may lead to poorly immunogenic viruses, thus a different LAV strategy based on viruses keeping the NSs but including additional combinations of single attenuation changes may be preferred [29]. In this case, the P82L substitution could be included as an additional safety feature, since our results show that it does not affect the viral growth (production) or immunogenicity. Of note, the mutation P82L was found in a virus derived from a South African origin (lineage D) [30]. Here we report the biological consequences of this change in the context of the ZH548 backbone (lineage A) stressing the relevance of amino acid residue 82 among distinct RVFV lineages).

On the other hand, how this single change in the NSs leads to in vivo attenuation remains unknown. Except for a tenuous difference in the consistency and definition of the nuclear filaments, all other NSs features analyzed in this work known to affect virulence did not show significant differences between the virulent rZH548 and the mutant viruses. Virus growth and yield in Vero cells were equivalent and the rZH548-mut S279 viruses retained the ability to block IFN production in IFN-competent cells and to degrade cellular PKR and p62. Interactions of NSs with other cellular proteins related with mitochondrial or nuclear targeting or further interfering with the host antiviral response, as well as other effects influencing apoptosis or different immunological pathways, may contribute to the attenuated phenotype observed in mice. Work is in progress to determine the pathway affected by the substitution P82L studied in this work

Author Contributions: Conceptualization, B.B. and A.B.; methodology, B.B., S.M., and NdL; validation, S.M., NdL. and B.B.; formal analysis, B.B. and A.B; investigation, B.B. and S.M; resources, A.B. S.M. F.W.; data curation, B.B. and S.M.; writing—original draft preparation, B.B.; writing—review and editing, F.W. and A.B.; visualization, B.B. and A.B.; supervision, A.B.; project administration, A.B.; funding acquisition, B.B. and A.B. All authors have read and agreed to the published version of the manuscript.

Funding: This research was funded by grants S2013/ABI-2906 (PLATESA), P2018/BAA-4370 (PLATESA2) from Comunidad de Madrid and AGL2017-83226-R from Ministerio de Ciencia e Innovación. The APC was funded by grant AGL2017-83226-R. FW was supported by the Deutsche Forschungsgemeinschaft (DFG; German Research Foundation) (project number 197785619–SFB 1021) and the Swedish Research Council (VR; no. 2018-05766).

Institutional Review Board Statement: The study was conducted according to the guidelines of the Declaration of Helsinki, and approved by the Animal Care and Biosafety Ethics' Committees of INIA and Comunidad de Madrid (permit codes CEEA 2014/26, CBS 2017/15, PROEX 108/15 and PROEX192/17)

Acknowledgments: We thank the Optical and Confocal Microscopy Unit at Centro de Biología Molecular Severo Ochoa (CBMSO, Madrid) for support with confocal image analysis. We also thank Dr Martin Eiden (FLI, Insel Riems) for supplying of NSs-specific monoclonal antibodies.

Conflicts of Interest: "The authors declare no conflict of interest."

References

1. Ikegami, T.; Makino, S. The pathogenesis of Rift Valley fever. *Viruses* **2011**, *3*, 493-519, doi:10.3390/v3050493.
2. Rolin, A.I.; Berrang-Ford, L.; Kulkarni, M.A. The risk of Rift Valley fever virus introduction and establishment in the United States and European Union. *Emerg Microbes Infect* **2013**, *2*, e81, doi:10.1038/emi.2013.81.
3. Boshra, H.; Lorenzo, G.; Busquets, N.; Brun, A. Rift valley fever: recent insights into pathogenesis and prevention. *J Virol* **2011**, *85*, 6098-6105, doi:JVI.02641-10 [pii]
10.1128/JVI.02641-10.
4. Kortekaas, J. One Health approach to Rift Valley fever vaccine development. *Antiviral Res* **2014**, *106*, 24-32, doi:S0166-3542(14)00082-5 [pii]
10.1016/j.antiviral.2014.03.008.
5. Faburay, B.; LaBeaud, A.D.; McVey, D.S.; Wilson, W.C.; Richt, J.A. Current Status of Rift Valley Fever Vaccine Development. *Vaccines (Basel)* **2017**, *5*, doi:E29 [pii]
10.3390/vaccines5030029
vaccines5030029 [pii].
6. Kreher, F.; Tamietti, C.; Gommet, C.; Guillemot, L.; Ermonval, M.; Failloux, A.B.; Panthier, J.J.; Bouloy, M.; Flamand, M. The Rift Valley fever accessory proteins NSm and P78/NSm-GN are distinct determinants of virus propagation in vertebrate and invertebrate hosts. *Emerg Microbes Infect* **2014**, *3*, e71, doi:10.1038/emi.2014.71.
7. Weingartl, H.M.; Zhang, S.; Marszal, P.; McGreevy, A.; Burton, L.; Wilson, W.C. Rift Valley fever virus incorporates the 78 kDa glycoprotein into virions matured in mosquito C6/36 cells. *PLoS One* **2014**, *9*, e87385, doi:10.1371/journal.pone.0087385
PONE-D-13-31002 [pii].
8. Ly, H.J.; Ikegami, T. Rift Valley fever virus NSs protein functions and the similarity to other bunyavirus NSs proteins. *Virol J* **2016**, *13*, 118, doi:10.1186/s12985-016-0573-8
10.1186/s12985-016-0573-8 [pii].
9. Wuerth, J.D.; Weber, F. Phleboviruses and the Type I Interferon Response. *Viruses* **2016**, *8*, doi:10.3390/v8060174
E174 [pii]
v8060174 [pii].
10. Narayanan, A.; Amaya, M.; Voss, K.; Chung, M.; Benedict, A.; Sampey, G.; Kehn-Hall, K.; Luchini, A.; Liotta, L.; Bailey, C., et al. Reactive oxygen species activate NFkappaB (p65) and p53 and induce apoptosis in RVFV infected liver cells. *Virology* **2014**, *449*, 270-286, doi:10.1016/j.virol.2013.11.023
S0042-6822(13)00645-4 [pii].
11. Barski, M.; Brennan, B.; Miller, O.K.; Potter, J.A.; Vijayakrishnan, S.; Bhella, D.; Naismith, J.H.; Elliott, R.M.; Schwarz-Linek, U. Rift Valley fever phlebovirus NSs protein core domain structure suggests molecular basis for nuclear filaments. *Elife* **2017**, *6*, doi:10.7554/eLife.29236
e29236 [pii].
12. Head, J.A.; Kalveram, B.; Ikegami, T. Functional analysis of Rift Valley fever virus NSs encoding a partial truncation. *PLoS One* **2012**, *7*, e45730, doi:10.1371/journal.pone.0045730
PONE-D-12-19679 [pii].
13. Leger, P.; Nachman, E.; Richter, K.; Tamietti, C.; Koch, J.; Burk, R.; Kummer, S.; Xin, Q.; Stanifer, M.; Bouloy, M., et al. NSs amyloid formation is associated with the virulence of Rift Valley fever virus in mice. *Nat Commun* **2020**, *11*, 3281, doi:10.1038/s41467-020-17101-y
10.1038/s41467-020-17101-y [pii].
14. Borrego, B.; Brun, A. A hyper-attenuated variant of Rift Valley fever virus (RVFV) generated by a mutagenic drug (favipiravir) unveils potential virulence markers *Frontiers in Microbiology (submitted)* **2020**.
15. Billecocq, A.; Spiegel, M.; Vialat, P.; Kohl, A.; Weber, F.; Bouloy, M.; Haller, O. NSs protein of Rift Valley fever virus blocks interferon production by inhibiting host gene transcription. *J Virol* **2004**, *78*, 9798-9806, doi:10.1128/JVI.78.18.9798-9806.2004
78/18/9798 [pii].
16. Moreno, S.; Calvo-Pinilla, E.; Devignot, S.; Weber, F.; Ortego, J.; Brun, A. Recombinant Rift Valley fever viruses encoding bluetongue virus (BTV) antigens: Immunity and efficacy studies upon a BTV-4 challenge. *PLoS Negl Trop Dis* **2020**, *14*, e0008942, doi:10.1371/journal.pntd.0008942

PNTD-D-20-00574 [pii].
17. Habjan, M.; Penski, N.; Spiegel, M.; Weber, F. T7 RNA polymerase-dependent and -independent systems for cDNA-based rescue of Rift Valley fever virus. *J Gen Virol* **2008**, *89*, 2157-2166, doi:89/9/2157 [pii]
10.1099/vir.0.2008/002097-0.
18. Lopez-Gil, E.; Moreno, S.; Ortego, J.; Borrego, B.; Lorenzo, G.; Brun, A. MVA Vectored Vaccines Encoding Rift Valley Fever Virus Glycoproteins Protect Mice against Lethal Challenge in the Absence of Neutralizing Antibody Responses. *Vaccines (Basel)* **2020**, *8*, doi:E82 [pii]
10.3390/vaccines8010082
vaccines8010082 [pii].
19. Mwaengo, D.; Lorenzo, G.; Iglesias, J.; Warigia, M.; Sang, R.; Bishop, R.P.; Brun, A. Detection and identification of Rift Valley fever virus in mosquito vectors by quantitative real-time PCR. *Virus Res* **2012**, *169*, 137-143, doi:S0168-1702(12)00285-7 [pii]
10.1016/j.virusres.2012.07.019.
20. Mroz, C.; Schmidt, K.M.; Reiche, S.; Groschup, M.H.; Eiden, M. Development of monoclonal antibodies to Rift Valley Fever Virus and their application in antigen detection and indirect immunofluorescence. *J Immunol Methods* **2018**, *460*, 36-44, doi:S0022-1759(18)30091-7 [pii]
10.1016/j.jim.2018.06.006.
21. Muller, R.; Saluzzo, J.F.; Lopez, N.; Dreier, T.; Turell, M.; Smith, J.; Bouloy, M. Characterization of clone 13, a naturally attenuated avirulent isolate of Rift Valley fever virus, which is altered in the small segment. *Am J Trop Med Hyg* **1995**, *53*, 405-411.
22. Bouloy, M.; Janzen, C.; Vialat, P.; Khun, H.; Pavlovic, J.; Huerre, M.; Haller, O. Genetic evidence for an interferon-antagonistic function of rift valley fever virus nonstructural protein NSs. *J Virol* **2001**, *75*, 1371-1377, doi:10.1128/JVI.75.3.1371-1377.2001.
23. Habjan, M.; Pichlmair, A.; Elliott, R.M.; Overby, A.K.; Glatter, T.; Gstaiger, M.; Superti-Furga, G.; Unger, H.; Weber, F. NSs protein of rift valley fever virus induces the specific degradation of the double-stranded RNA-dependent protein kinase. *J Virol* **2009**, *83*, 4365-4375, doi:JVI.02148-08 [pii]
10.1128/JVI.02148-08.
24. Ikegami, T.; Narayanan, K.; Won, S.; Kamitani, W.; Peters, C.J.; Makino, S. Rift Valley fever virus NSs protein promotes post-transcriptional downregulation of protein kinase PKR and inhibits eIF2alpha phosphorylation. *PLoS Pathog* **2009**, *5*, e1000287, doi:10.1371/journal.ppat.1000287.
25. Kalveram, B.; Lihoradova, O.; Ikegami, T. NSs protein of rift valley fever virus promotes posttranslational downregulation of the TFIIH subunit p62. *J Virol* **2011**, *85*, 6234-6243, doi:JVI.02255-10 [pii]
10.1128/JVI.02255-10.
26. Borrego, B.; de Avila, A.I.; Domingo, E.; Brun, A. Lethal Mutagenesis of Rift Valley Fever Virus Induced by Favipiravir. *Antimicrob Agents Chemother* **2019**, *63*, doi:e00669-19 [pii]
10.1128/AAC.00669-19
AAC.00669-19 [pii].
27. Monteiro, G.E.R.; Jansen van Vuren, P.; Wichgers Schreur, P.J.; Odendaal, L.; Clift, S.J.; Kortekaas, J.; Paweska, J.T. Mutation of adjacent cysteine residues in the NSs protein of Rift Valley fever virus results in loss of virulence in mice. *Virus Res* **2018**, *249*, 31-44, doi:S0168-1702(18)30124-2 [pii]
10.1016/j.virusres.2018.03.005.
28. Li, S.; Zhu, X.; Guan, Z.; Huang, W.; Zhang, Y.; Kortekaas, J.; Lozach, P.Y.; Peng, K. NSs Filament Formation Is Important but Not Sufficient for RVFV Virulence In Vivo. *Viruses* **2019**, *11*, doi:E834 [pii]
10.3390/v11090834
v11090834 [pii].
29. Terasaki, K.; Juelich, T.L.; Smith, J.K.; Kalveram, B.; Perez, D.D.; Freiberg, A.N.; Makino, S. A single-cycle replicable Rift Valley fever phlebovirus vaccine carrying a mutated NSs confers full protection from lethal challenge in mice. *Sci Rep* **2018**, *8*, 17097, doi:10.1038/s41598-018-35472-7
10.1038/s41598-018-35472-7 [pii].
30. Bird, B.H.; Khristova, M.L.; Rollin, P.E.; Ksiazek, T.G.; Nichol, S.T. Complete genome analysis of 33 ecologically and biologically diverse Rift Valley fever virus strains reveals widespread virus movement and low genetic diversity due to recent common ancestry. *J Virol* **2007**, *81*, 2805-2816, doi:JVI.02095-06 [pii]
10.1128/JVI.02095-06.